RSC Advances

ROYAL SOCIETY
OF CHEMISTRY

www.rsc.org/advances

RSC Advances

RSC Advances

PAPER

Synthesis of ketoxime-functionalized Fe₃O₄@C core-shell magnetic microspheres for enhanced uranium (VI) removal

Qi Liu,[a] Wenting Li,[a] Wei Zhao,[c] Lichao Tan,[a, d] Xiaoyan Jing,[a] Jingyuan Liu,[a] Dalei Song,[a] Hongsen Zhang,[a] Rumin Li,*[a] Lianhe Liu,[b] and Jun Wang,*[a, b]

Ketoxime-functionalized carbon coated iron oxide (Fe₃O₄@C-KO) was synthesized and characterized by transmission electron microscopy, X-ray diffraction, Fourier transformed infrared spectroscopy, and magnetic measurements. The essential factors affecting
[10] uranium (VI) adsorption from aqueous solution of Fe₃O₄@C-KO, such as initial pH, contact time and temperature, were investigated. The adsorption is highly dependent on solution pH. The analysis of experimental data using sorption kinetic models, reveal that the process follows a pseudo-second-order kinetic model. In addition, adsorption isotherm and thermodynamics were investigated. The adsorption of uranium (VI) from aqueous solution onto Fe₃O₄@C-KO was fitted to Langmuir and Freundlich adsorption isotherms. The adsorption of uranium (VI) is well-described by the Langmuir isotherm. Thermodynamic parameters further show that the sorption is an
[15] endothermic and spontaneous process. Fe₃O₄@C-KO is a powerful and promising sorbent for the efficient removal of uranium (VI) from aqueous solutions.

Introduction

Due to the rapid development of modern industry, heavy metal
[20] ions have excessively accumulated in the biosphere and water, leading to a deterioration of the natural environment and a serious health hazard.[1,2] Uranium is a typical heavy metal element; it is radioactive and toxic.[3-5] Therefore, it is necessary to extract uranium from industrial waste water. Conventional methods for
[25] the removal of uranium include chemical precipitation,[6] solvent extraction,[7] ion-exchange,[8] ultrafiltration,[9] reverse osmosis and nanofiltration.[10] In comparison with these, adsorption techniques have several advantages[11–13] including low cost, ease of operation and high efficiency, and have become the predominant methods
[30] for the removal and recovery of uranium ions.

In adsorption, as the sorbent is a key factor, much attention has focused on researching new sorbents with fast sorption kinetics, high surface area and good stability for a wide pH range. Traditional sorbents such as oxides and clay material suffer from
[35] either low sorption efficiencies or low capacities.

Recently, numerous adsorbents have been developed; these include nanooxides, nanocarbon and carbon-based nanocomposites,[14-18] that exhibit excellent sorption capacity. However, the separation process of adsorbents from aqueous
[40] solutions after saturated adsorption is usually complex and time-consuming. Magnetic nanoparticles (MNPs), especially Fe₃O₄, have attracted more attention because of their outstanding properties, such as ease of separation and low toxicity.[19-22] Das et al. have studied the sorption of uranium (VI) onto magnetite
[45] (Fe₃O₄) nanoparticles, but the sorption capacity is relatively small. To increase the adsorption capacity, researchers have modified the

magnetic nanoparticles with other materials. Ketoxime, an excellent chelate functional group, has been grafted onto the surfaces of various substrates for recovery and removal of
[50] uranium (VI) to achieve fast sorption rate, high uranium (VI) loading capacity, and safety of the environment.[23-25]

Based on a high-throughput, one-pot solvothermal approach, Fe₃O₄@C nanoparticles (NPs) are synthesized and then modified with ketoxime (KO) on the surface (Fe₃O₄@C-KO). The prepared
[55] Fe₃O₄@C-KO was used to extract uranium (VI) from aqueous solutions, and the sorption kinetics, effects of geochemical conditions, sorption capability, stability and regeneration were investigated. Based on the experimental findings, the potential application of Fe₃O₄@C-KO for the recovery and removal of
[60] uranium (VI) was evaluated.

Experimental

Material Preparation

All the chemical reagents in this work are purchased from Tianjin Kermel Chemical Reagents Development and used without
[65] further purification. A solvothermal method was adopted [26, 27] and slightly modified to control particle size at around 100 nm. Briefly, ferrocene (0.15 g) was dissolved in 30 mL acetone with the aid of ultrasonication for 10 min. 0.5 mL H₂O₂ was slowly added, and the solution magnetically stirred for 30 min. After that,
[70] the precursor solution was transferred into a Teflon-lined stainless autoclave with a capacity of 50 mL. For the reaction, the temperature was maintained at 210 °C for 24 h, before cooling to room temperature naturally. The mixture in the autoclave was subjected to ultrasonic treatment for 10 min. The precipitates
[75] were collected by a magnet from the mixture and washed with

acetone three times.

Acetophenone (2.00 g) was dissolved in ethanol (55 mL) with stirring. $NH_2OH \cdot HCl$ (1.03 g, 1.48×10^{-2} mol) in 20 mL of water and Na_2CO_3 (0.78 g, 7.40×10^{-3} mol) in 20 mL of water were
5 added to the ethanolic acetophenone solution. The mixture was heated under reflux. With concentration of the solution, yellow, needle-shaped crystals precipitated from solution; these were collected via vacuum filtration and washed with cold water. [28]

$Fe_3O_4@C$ powder (0.1 g) was dried at 120 °C overnight and
10 mixed with 0.5 g of acetophenone oxime until a fine black powder was obtained. Then, 4 mL of isoamyl nitrite was added dropwise under vigorous stirring. The stirring was continued for 1 h at room temperature. The reaction mixture was then heated at 70 °C for 2 h before washing five times with dimethylformamide
15 (DMF) and three times with ethanol (EtOH). The resulting black powder was dried under a vacuum.[29]

Adsorption of uranium (VI)

Uranium removal experiments were performed in a series of conical flasks (100 mL) in which a given dose of the adsorbent
20 was shaken with uranium solution (50 mL), of given concentration and pH, in a thermostatic water shaker at speed of 200 rpm. The pH of the solution was adjusted with 0.5 M HNO_3 or NaOH solution. The mixture was shaken for 120 min in a thermostatic shaker bath. After magnetic separation, the
25 concentration of uranium (VI) in the solution was determined by Bruker 820-MS Inductive Coupled Plasma (ICP) instrument. The adsorption capacity Q_e (mg·g^{-1}) and the % removal of uranium were calculated according to Eqs. (1) and (2):

$$Q_e = \frac{(C_0 - C_e)V}{m} \tag{1}$$

$$Removal(\%) = \frac{100(C_0 - C_e)}{C_0} \tag{2}$$

where C_0 (mg·L^{-1}) is the uranium (VI) ion concentration in the initial solution, C_e (mg·L^{-1}) is the equilibrium concentration of
35 uranium (VI) ion in the supernatant, V (L) is the volume of the testing solution and m is the weight of sorbent (g).

Desorption studies

To investigate the reusability of $Fe_3O_4@C$-KO, 0.02 g of $Fe_3O_4@C$-KO was first put in contact with 20 mL uranium (VI)
40 for 120 min. After adsorption, desorption was carried out by washing the adsorbents with distilled water several times. Then the solution containing 20 mL different concentrations of HCl solution was added into the adsorbed uranium (VI) adsorbents for 120 min. After magnetic separation, the remaining uranium (VI)
45 concentration in the supernatant was measured to evaluate the desorption percentage. The regenerated $Fe_3O_4@C$-KO was washed thoroughly with distilled water and then used for the next sorption-desorption cycle.

Characterization

50 X-ray diffraction (XRD) analysis was performed on a Rigaku D/max-IIIB diffractometer with CuKα irradiation (Kα = 1.54178 Å). The X-ray source was operated at 40 kV and the current used in XRD measurements was 150 mA. Morphology was

characterized using Transmission electron microscopy(TEM).
55 Powder samples for the TEM observation were dispersed in ethanol by ultrasound and mounted onto a carbon-coated copper microgrid. TEM images were taken by TEM (FEI Tecnai G2 S-Twin) with an acceleration voltage of 200 kV. The magnetic measurement was carried out with a vibrating sample
60 magnetometer (VSM, Lanzhou University LakeShore 7304). Effluent was analyzed using WGJ–III Trace Uranium Analyzer from the Bruker 820-MS ICP instrument.

Results and discussion

Characterization of samples

65 Fig. 1 shows the XRD patterns of as-synthesized $Fe_3O_4@C$-KO. In the XRD pattern of $Fe_3O_4@C$-KO (Fig. 1), we see that the diffraction peaks correspond to the (220), (311), (400), (422), (511), (440) and (622) crystalline planes of cubic Fe_3O_4 (JCPDS75-1609), validating the presence of Fe_3O_4 nanocrystals
70 within the core-shell structure. The broad band around 22º is ascribed to amorphous carbon,[30] which indicates that the core-shell microspheres have been successfully synthesized.
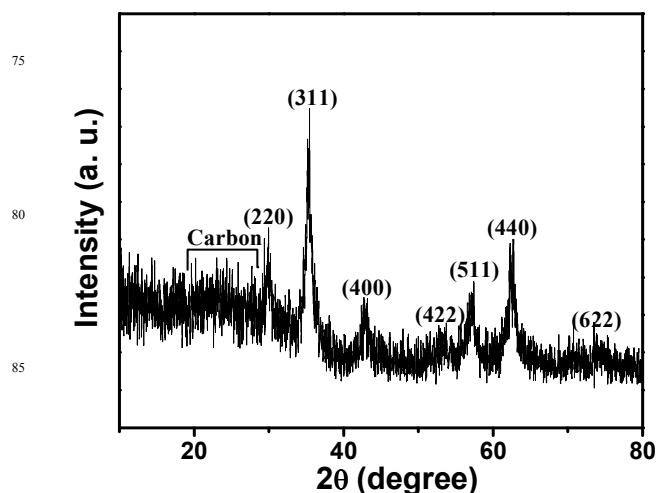

Fig. 1 XRD patterns of $Fe_3O_4@C$-KO.

The magnetic properties of $Fe_3O_4@C$-KO were studied at room temperature by measuring the magnetization curves, as shown in Fig. 2. The saturation magnetization (Ms) value is 30.33 emu·g^{-1} for $Fe_3O_4@C$-KO. Although the saturation magnetization
95 decreases due to the decrease of the magnetite fraction after carbon coating,[31, 32] complete magnetic separation is quickly achieved by placing a magnet near the vessels containing the aqueous dispersion of $Fe_3O_4@C$-KO particles.

To identify the modification with ketoxime functional groups,
100 FT-IR spectra of $Fe_3O_4@C$ and $Fe_3O_4@C$-KO were recorded (Fig. 3). The peak at 588 cm^{-1} is attributed to the stretching vibration of the Fe-O bond (Fig. 3 $Fe_3O_4@C$). The broad band around 3180 cm^{-1} corresponds to -OH stretching vibration, and the band around 1720 cm^{-1} corresponds to the bending vibration of C=O,[33]
105 reflecting the coating of carbon on the magnetite surface (Fig. 3 $Fe_3O_4@C$). After modification with KO (Fig. 3 $Fe_3O_4@C$-KO), the C=O absorption bands disappear while two new bands arise at 1658 cm^{-1} and 1010 cm^{-1} corresponding to the C=N and N-O

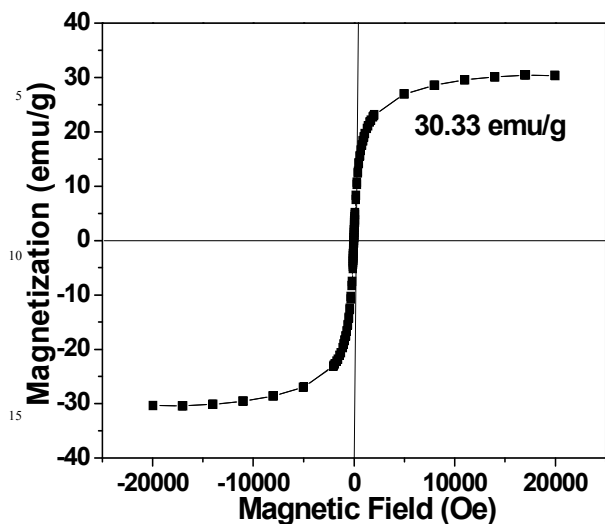stretching vibrations of ketoxime groups, respectively.[34]

Fig. 2 Magnetic hysteresis loop for Fe$_3$O$_4$@C-KO at 300 K.

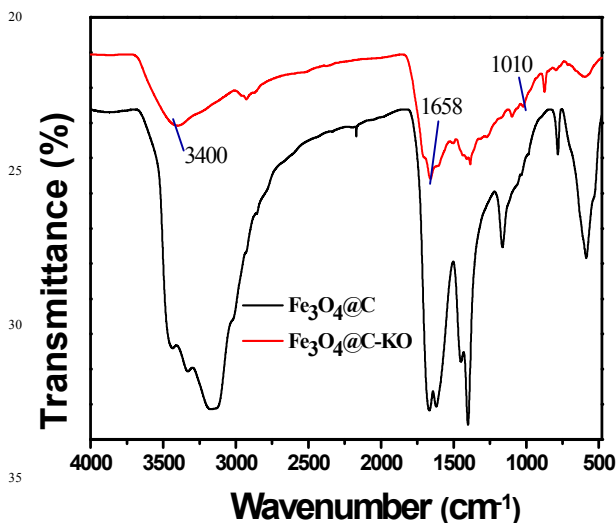**Fig. 3** FT-IR spectra of Fe$_3$O$_4$@C and Fe$_3$O$_4$@C-KO.

The mophology of Fe$_3$O$_4$@C and Fe$_3$O$_4$@C-KO were characterized by TEM, which shows in Fig. 4A and 4B that the obtained Fe$_3$O$_4$@C product is composed of spherical nanoparticles with an average diameter of about 90 nm. As shown in Fig. 4A, the condensation of carbon onto the surfaces of Fe$_3$O$_4$ cores results in microspheres with dark-colored Fe$_3$O$_4$ cores and gray-colored carbon shells having an average thickness of about 30 nm. The clarity of the core-shell structure is due to the distinct density contrast between these two components. The HRTEM image (Figure. 4C) shows a clear lattice between the adjacent fringes. The lattice *d*-spacing of 0.29 nm corresponding to (220) planes of Fe$_3$O$_4$, is identified in Fig. 4C. The selected area electron diffraction (SAED) pattern (Fig. 4D) obtained from this core-shell structure has a highly symmetrical dotted lattice, which reveals the single-crystalline nature of Fe$_3$O$_4$. To further investigate their microstructure, elemental mapping was employed to investigate the TEM elemental distributions in the unique core–shell structure, as depicted in Fig. 5, which reveals a uniform distribution of Fe, O, C and N.
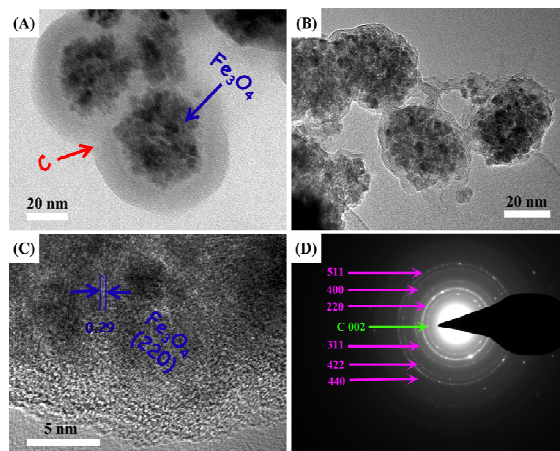

Fig. 4 TEM image of Fe$_3$O$_4$@C ((A)), TEM image, HRTEM image and SAED pattern of Fe$_3$O$_4$@C-KO ((B), (C) and (D)).

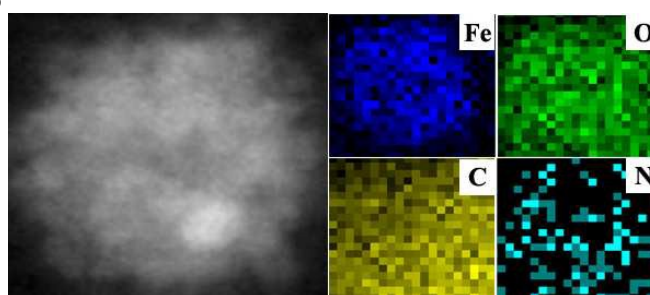**Fig. 5** TEM elemental mappings of Fe$_3$O$_4$@C-KO.

Effect of pH on the uranium (VI) adsorption

The pH for the adsorbate solution plays an important role in sorption studies. To study the effect of the uranium (VI) sorption onto Fe$_3$O$_4$@C-KO, a number of batch extraction experiments were carried out in which the pH of the working solution varied from 2 to 12 for 120 min contact time at room temperature. The results in Fig. 6 show that UO$_2^{2+}$ adsorption capacity increases with the increase in pH from 2.0 to 6.0. At a pH of 2.0, the adsorption effect is very weak because of effective competition between high concentrations of H$^+$ and H$_3$O$^+$.[35]
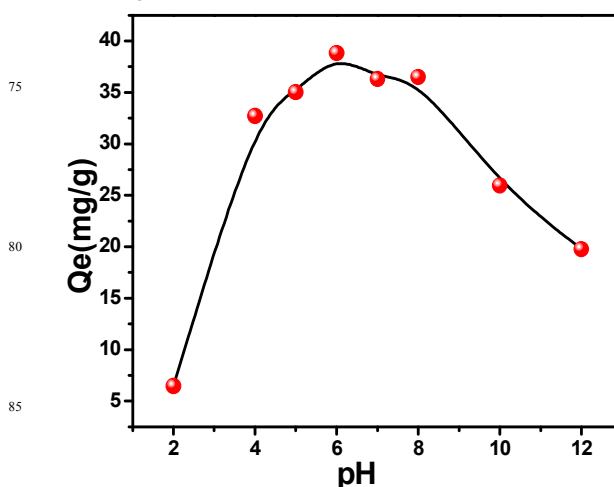

Fig. 6 Effect of initial pH on adsorption of uranium by Fe$_3$O$_4$@C-KO. (Adsorption dosage 0.02 g, retention time 120 min, T = 25

°C and pH = 2 ~ 12)

The adsorption capacity reaches a maximum at pH 6.0 and diminishes as the pH rises from 6.0 to 12.0. With a pH higher than 6.0, uranium is present in an anionic form by complexation with carbonate and hydroxyl anions[36,37] which has less interaction with functional groups of Fe_3O_4@C-KO leading to a decrease in adsorption. Consequently, pH 6.0 is considered as the optimum pH for further experiments.

Effect of contact time on uranium sorption

Since the contact time between the adsorbate and adsorbent is a key parameter for the adsorption process, the effect of contact time on adsorption of uranium (VI) onto Fe_3O_4@C-KO was investigated to determine the equilibrium point. The adsorption experiments were carried out for contact times ranging from 15 to 480 min, with 20 mg adsorbents and 20 mL of 50 mg/L uranium (VI) solution at 25°C, and with an initial pH of 6.0 for Fe_3O_4@C-KO. We observe that uranium (VI) uptake increases sharply in the first 60 min, and does not change significantly after 120 min (Fig. 7). Uranium (VI) adsorption achieves an equilibrium around 120 min. We interpret from the initial rapid adsorption of uranium (VI) that Fe_3O_4@C-KO has a high specific surface area and relatively large pore sizes; as a result, a shaking time of 120 min is appropriate for maximum sorption of uranium (VI) onto Fe_3O_4@C-KO.

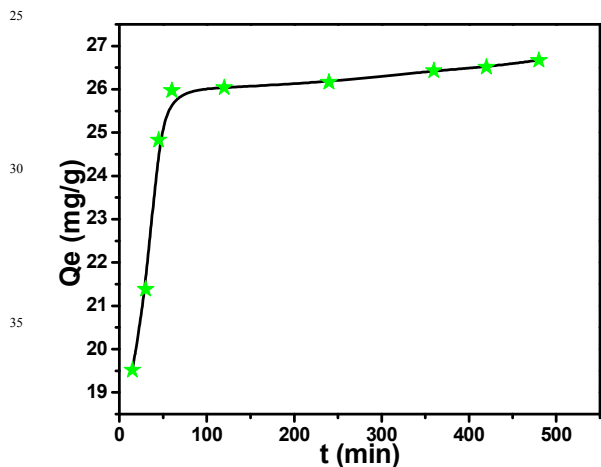**Fig. 7** Effect of reaction time on the adsorption of uranium by Fe_3O_4@C-KO. (Adsorption dosage 0.02 g, reaction time 5 min ~ 300 min, T = 25 ~ 55 °C and pH = 6)

Adsorption kinetics

To investigate the kinetic mechanism, which controls the adsorption process, the kinetics of uranium (VI) adsorption was modeled using pseudo-first-order and second-order rate equations. The first-order equation is written as:

$$\ln\left(q_e - q_t\right) = \ln q_e - k_1 t \tag{3}$$

where k_1 is the rate constant of pseudo-first-order adsorption, q_e and q_t (mg·g⁻¹) is the amount of uranium adsorbed at equilibrium and at time (t), respectively.

And the pseudo-second-order equation [38] is given as:

$$t/q_t = 1/k_2 \cdot q_e^2 + t/q_e \tag{4}$$

where k_2 is the rate constant of pseudo-second-order adsorption. By plotting ln $(q_e - q_t)$ versus t, the values of k_1 and q_e in pseudo-first-order equation are obtained from the slope and intercept (Fig. 8A), and by the same method, k_2 and q_e in pseudo-second-order equation are obtained (Fig. 8B). The calculated kinetic parameters from both model fittings are shown in Table 1.

In pseudo-second-order kinetics, the calculated q_e values are nearly the same as the experimental values, and the regression coefficient is 0.9998, which confirms that the adsorption of uranium (VI) ions adsorption onto Fe_3O_4@C-KO is described by a pseudo-second-order model. These results suggest that a pseudo-second-order adsorption is the predominant mechanism and the rate constant of uranium (VI) ions appears to be controlled by a chemisorption process.
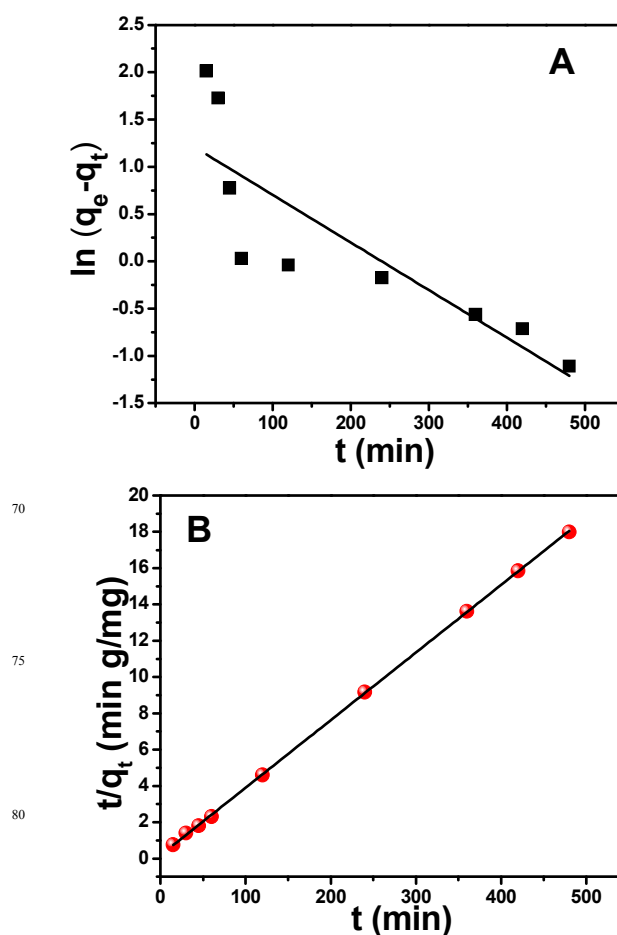

Fig. 8 Pseudo-first-order kinetics and Pseudo-second-order kinetics for removal of uranium by Fe_3O_4@C-KO.

Table 1 Kinetic parameters for adsorption of uranium on Fe_3O_4@C-KO.

Kinetic model	T (°C)	C_0 (mg/L)	Q_e^{exp} (mg/g)	Q_e^{cal} (mg/g)	k_1(min⁻¹)$/k_2$ (g/mg·min)	R^2

Pseudo-first order	25	60	27	3.34	0.0051	0.6893
Pseudo-second order	25	60	27	26.88	0.0076	0.9998

Effect of temperature and adsorption thermodynamics

The effect of temperature on uranium (VI) sorption onto Fe_3O_4@C-KO was investigated using a water bath with 20 mg adsorbent, 20 mL of uranium (VI) 50 mg/L, 120 min contact time,
5 and pH of 6.0 for Fe_3O_4@C-KO. The sorption of uranium (VI) onto Fe_3O_4@C-KO is highest at 328 K the lowest at 298 K (Fig. 9), indicating that high temperature is advantageous for uranium (VI) sorption.

Entropy ($\Delta S°$) and enthalpy ($\Delta H°$) changes, were calculated
10 using the following equation:[39]

$$\ln K_d = -\Delta H^0 / RT + \Delta S^0 / R \qquad (5)$$

where K_d is the equilibrium constant (mL·g⁻¹), $\Delta H°$ is standard enthalpy (kJ·mol⁻¹), $\Delta S°$ is standard entropy (J·mol⁻¹·K⁻¹), T is the absolute temperature (K), and R is the gas constant (8.314 J·mol⁻¹·K⁻¹).
15 The values of $\Delta H°$ and $\Delta S°$ are evaluated from the intercept and slope of the linear plot of ln K_d vs. $1/T$ (Fig. 10). The positive standard entropy ($\Delta S°$) means that randomness is increases at the solid/solution interface during adsorption. The positive value of $\Delta H°$ indicates the adsorption process of UO_2^{2+} is
20 endothermic.

The thermodynamic parameter, $\Delta G°$, is calculated from the following Gibbs–Helmholtz equation:

$$\Delta G^0 = \Delta H^0 - T \cdot \Delta S^0 \qquad (6)$$

where $\Delta G°$ is the standard Gibbs free energy. From Eq. (6), the
25 data of $\Delta G°$ at different temperatures are obtained. The data of $\Delta G°$, $\Delta H°$ and $\Delta S°$ are shown in Table 2. The negative values of $\Delta G°$ indicate that the adsorption follows a spontaneous and feasible trend. Gibbs free energy decreases with increase in temperature, which suggests that higher temperatures facilitate
30 adsorption of uranium (VI) ions onto Fe_3O_4@C-KO due to a greater driving force.

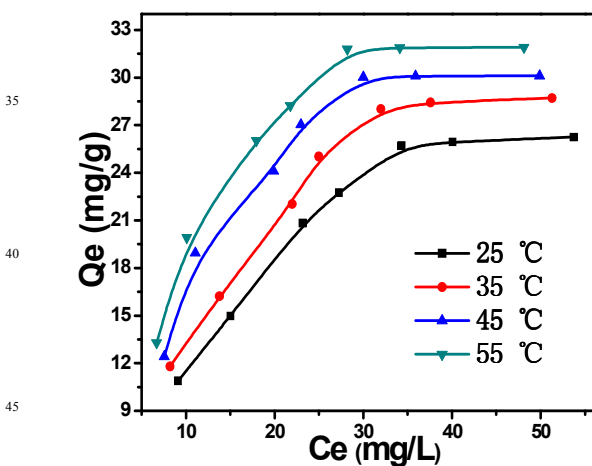**Fig. 9** Effect of uranium concentration on the adsorption of uranium by Fe_3O_4@C-KO. (Adsorption dosage 0.02 g, reaction

50 time 120 min, T = 25 ~ 55 °C and pH = 6)

Table 2 Thermodynamic parameters for adsorption of uranium on Fe_3O_4@C-KO.

$\Delta H°$ (kJ·mol⁻¹)	$\Delta S°$ (J·mol⁻¹·K⁻¹)	$\Delta G°$ (kJ·mol⁻¹)			
		298K	308K	318K	328K
10.21	40.43	-1.76	-2.24	-2.65	-3.05

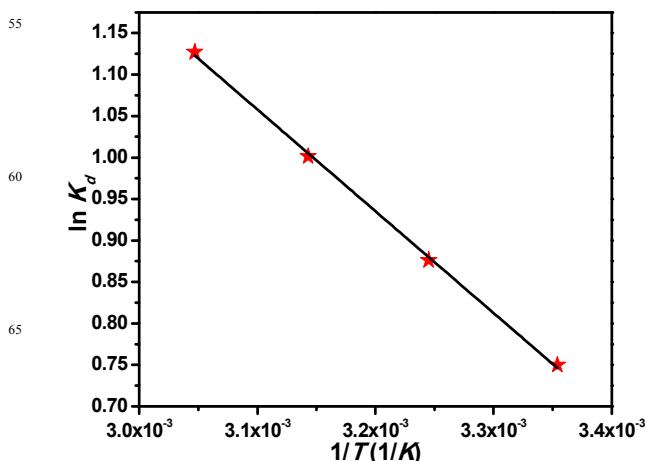70 **Fig. 10** Van 't Hoff plot for removal of uranium by Fe_3O_4@C-KO

Adsorption isotherms

For the design and operation of adsorption systems, correlation of equilibrium adsorption data is important. Langmuir and Freundlich isotherms models were applied to the obtained
75 adsorption data.

The Langmuir equation has been used extensively for dilute solutions in the following form: [40]

$$C_e / q_e = 1 / b \cdot q_m + C_e / q_m \qquad (7)$$

where C_e (mg·L⁻¹) is the equilibrium concentration of UO_2^{2+}
80 remained in solution, q_e (mg·g⁻¹) is the amount of solution adsorbed per unit mass of the adsorbent, q_m (mg·g⁻¹) is the maximum adsorption capacity, b is the Langmuir adsorption equilibrium constant. According to Eq. (7), a straight line is obtained and presented in Fig. 11A. The values of q_m and b are
85 calculated from the slope and the intercept, and are given in Table 3.

The Freundlich model is based on a reversible heterogeneous adsorption since it is not restricted to monolayer adsorption capacity.[38]
90 The Freundlich isotherm is given as:

$$\ln q_e = \ln K_f + n \ln C_e \qquad (8)$$

where k and n are the Freundlich constants related to the adsorption capacity and adsorption intensity, respectively. They are determined from the intercept and slope of the linear plot of ln
95 q_e vs. ln C_e (Fig. 11B).

The corresponding Langmuir and Freundlich parameters, along with the correlation coefficients, are reported in Table 3.

Table 3 shows that the Langmuir isotherm model better fits the experimental results over the experimental range, with high correlation coefficients (>0.95). The Langmuir model indicates that it is monolayer adsorption onto structurally homogeneous Fe$_3$O$_4$@C-KO. The maximum adsorption capacity of Fe$_3$O$_4$@C-KO is evaluated as 38.76 mg U/g at 25 ^{o}C.
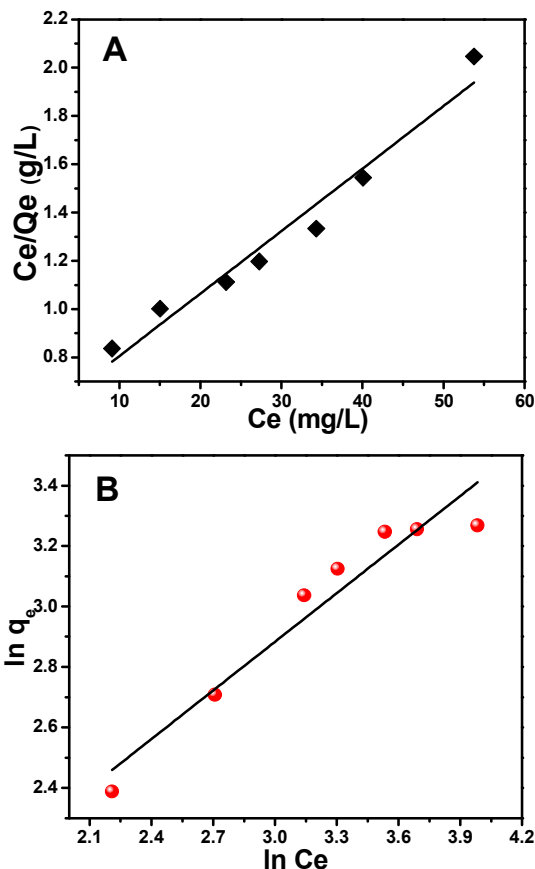

Fig. 11 Langmuir and Freundlich isotherm for removal of uranium by Fe$_3$O$_4$@C-KO

Table 3 Langmuir and Freundlich isotherm parameters for adsorption of uranium on Fe$_3$O$_4$@C-KO

Parameter	Value	R^2
Langmuir isotherm Q_m(mg·g^{-1})	38.76	0.9567
b (L·mg^{-1})	0.0472	
Freundlich isotherm K(L·g^{-1})	3.578	0.9222
n	1.866	-

Desorption and reusability study

To test the feasibility of Fe$_3$O$_4$@C-KO materials to be regenerated after adsorption of uranium (VI) ions, desorption was carried out with Fe$_3$O$_4$@C-KO adsorbent. Uranium (VI)-loaded adsorbent was regenerated using HCl solution. Various concentrations of HCl ranging between 0.01 and 1.0 M were tested for elution of adsorbed uranium (VI) ions using Fe$_3$O$_4$@C-KO. The percentage desorption of HCl concentrations of 0.01, 0.05, 0.1, 0.5 and 1.0 M is 68.0%, 75.0%, 78.0%, 87.0%, 87.1%, respectively. Therefore, the best and optimum concentration of HCl is determined as 0.5 M in terms of economic efficiency.

To assess the reusability of the adsorbent, the adsorption-desorption experiment with 0.5 M HCl was repeated for three cycles. After three cycles, the desorption efficiency of the Fe$_3$O$_4$@C-KO is still more than 80%. This result shows that the adsorbent can be used efficiently in a real process such as nuclear industry wastewater treatment.

Comparison of adsorbent performance with literature data

The removal of uranium (VI) by different adsorbents has been studied extensively. Table 4 represents the comparison of the adsorption capacity of uranium (VI) with other materials.[41-45] Adsorption capacity of Fe$_3$O$_4$@C-KO equal to 38.76 mg U/g is higher than that of other adsorbents, except for Oxime-grafted CMK-5. This data suggests that the Fe$_3$O$_4$@C-KO as adsorbent is suitable for the removal of uranium (VI) from aqueous solution.

Table 4 Comparison of the uranium (VI) sorption capacity of Fe$_3$O$_4$@C-KO with other sorbents.

Sorbents	Capacity (mg U/g)	Ref
Hematite	3.36	41
Functionalized polymer-coated silica	5.2	42
Amine modified silica gel	21.4	43
Activated carbon	28.3	44
Oxime-grafted CMK-5	62	45
Fe$_3$O$_4$@C-KO	38.7	Present work

Conclusions

A novel magnetic Fe$_3$O$_4$@C-KO composite has been fabricated, with its structure well-characterized by FT-IR, XRD, TEM and VSM. The adsorption process is pH dependent and accomplished within 120 min. The adsorption kinetic process is well-described by a pseudo-second-order model. Thermodynamic studies indicate an endothermic and spontaneous adsorption process. In addition, uranium (VI)-loaded Fe$_3$O$_4$@C-KO is easily separated from aqueous solutions by a magnet and efficiently renewed by HCl. The ease of operation and fast and efficient adsorption performance indicate that Fe$_3$O$_4$@C-KO can be used as a highly effective material for the removal of uranium (VI) ions from aqueous solution.

Notes and references

ᵃ Key Laboratory of Superlight Material and Surface Technology, Ministry of Education, Harbin Engineering University, Harbin 150001, China. Fax: +86 451 8253 3026; Tel: +86 451 8253 3026; E-mail address: zhqw1888@sohu.com
ᵇ Institute of Advanced Marine Materials, Harbin Engineering University, 150001, China.
ᶜInstitute of Scientific and Technical Information of Heilongjiang Province. Harbin 150028, China.
ᵈKey Laboratory of Green Chemical Engineering and Technology of College of Heilongjiang Province, College of Chemical and Environmental Engineering, Harbin University of Science and Technology, Harbin 150040, China.

1. S. J. DeCanio and A. Fremstad, *Energ. Policy.,* 2011, 39, 1144–1153.
2. B. Volesky, Z. R. Holan, Biotechnol. Prog., 1995, 11, 235-250.
3. H. Nifenecker, Future electricity production methods. Part 1:Nuclear energy. Rep. Prog. Phys., 2011, 74 (2), 1–28.
4. M. Asif, T. Muneer, Renewable and Sustainable Energy Rev., 2007, 11(7), 1388–1413.
5. Y. Lu, Nature chemistry, 2014, 6, 175–177.
6. A.E. Santos and A.C.Q. Ladeira, *Environ. Sci. Technol.,* 2011, 45, 3591–3597.
7. M. Koh, J. Yoo, Y. Park, D. Bae, K. Park, H. Kim, and H. Kim, *Ind. Eng. Chem. Res.,* 2006, 45, 5308–5313.
8. S.Y. Bae, G.L. Southard, and G.M. Murray, *Anal. Chim. Acta,* 1999, 397, 173–181.
9. A. J. C. Semiao, H. M. A. Rossiter, and A. I. Schafer, *J. Membrane Sci.,* 2010, 348, 174–180.
10. M.G. Khedr, *Desalination.,* 2013, 321, 47–54.
11. M. Hua, S. Zhang, B. Pan, W. Zhang, L. Lv, and Q. Zhang, *J. Hazard Mater.,* 2012, 317, 211–212.
12. Y. Ni, L. Jin, L. Zhang, and J. Hong, *J. Mater. Chem.,* 2010, 20, 6430–6436.
13. A. Tripathi, J. S. Melo, and S. F. D'Souza, *J. Hazard. Mater.,* 2013, 246, 87–95.
14. G.X. Zhao, L. Jiang, Y.D. He, J.X. Li, H.L. Dong, X.K. Wang, W.P. Hu, Adv. Mater., 2011, 23, 3959–3963.
15. Y.B. Sun, S.T. Yang, G.D. Sheng, Z.Q. Guo, X.L. Tan, J.Z. Xu, X.K. Wang, Sep. Purif. Technol., 2011, 83, 196–203.
16. D.D. Shao, Z.Q. Jiang, X.K. Wang, J.X. Li, Y.D. Meng, J. Phys. Chem. B, 2009, 113, 860–864.
17. H. Chen, J.X. Li, D.D. Shao, X.M. Ren, X.K. Wang, Chem. Eng. J., 2012, 210, 475–481.
18. J.X. Li, S.Y. Chen, G.D. Sheng, J. Hu, X.L. Tan, X.K. Wang, Chem. Eng. J., 2011, 166, 551–558.
19. V. Chandra, J. Park, Y. Chun, J.W. Lee, I.C. Hwang, K.S. Kim, ACS Nano, 2010, 4, 3979–3986.
20. I. Akin, G. Arslan, A. Tor, M. Ersoz, Y. Cengeloglu, J. Hazard. Mater., 2012, 235, 62–68.
21. H.Y. Koo, H.J. Lee, H.A. Go, Y.B. Lee, T.S. Bae, J.K. Kim, W.S. Choi, Chem. Eur. J., 2011, 17, 1214–1219.
22. J.X. Li, Z.Q. Guo, S.W. Zhang, X.K. Wang, Chem. Eng. J., 2011, 172, 892–897.
23. S. Das, A.K. Pandey, A.A. Athawale, V.K. Manchanda, J. Phys. Chem. B, 2009, 113, 6328–6335.
24. O. Hazer, S. Kartal, Talanta, 2010, 82, 1974–1979.
25. A.Y. Zhang, G. Uchiyama, T. Asakura, React. Funct. Polym., 2005, 63, 143–153.
26. Q. An, M. Yu, Y.T. Zhang, W.F. Ma, J. Guo, C.C. Wang, J. Phys. Chem. C 2012, 116, 22432-22440.
27. Q. An, P. Zhang, J.M. Li, W.F. Ma, J. Guo, J. Hu, C.C. Wang, Nanoscale, 2012, 4, 5210-5216.
28. B. Christer, Y. Aakero, M. Alicia, S. Destin, Crystal Growth & Design, 2001, 1, 47-52.
29. M. Carboni, C.W. Abney, M. L. Kathryn, L. Juan, V. Escoto, and W.B. Lin, Industrial & Engineering Chemistry Research, 2013, 52, 15187-15197.
30. U. Kalapathy, A. Proctor, J. Shultz, Bioresour. Technol. 2000, 73, 257–262.
31. J.H. Wang, S.R. Zheng, Y. Shao, J.L. Liu, Z.Y. Xu, D.Q. Zhu, J. Colloid Interface Sci. 2010, 349, 293–299.
32. S.H. Xuan, L.Y. Hao, W.Q. Jiang, X.L. Gong, Y. Hu, Z.Y. Chen, Nanotechnology, 2007, 18, 035602.
33. S. Sadeghi, H. Azhdari, H. Arabi, A.Z. Moghaddam, J. Hazard. Mater. 2012, 215, 208–216.
34. B.J. Gao, Y.C. Gao, Y.B. Li, Chem. Eng. J., 2010, 158, 542–549.
35. A. Schierz, H. Zaker, Environ. Pollut. 2009, 157, 1088–1094.
36. M. Sutton, S.R. Burastero, Chem. Res. Toxicol., 2004, 17, 1468–1480.
37. M. Wazne, G.P. Korfiatis, and X.G. Meng, Environ. Sci. Technol., 2003, 37, 3619-3624.
38. Y. S. Ho, G. McKay, Water. Res. 2000, 34, 735–742.
39. G. Moussavi, R. Khosravi, Chem. Eng. Res. Des., 2011, 89, 2182–2189.
40. I. Langmuir, J. Am. Chem. Soc. 1918, 40, 1361–1403.
41. A. Mellah, S. Chegrouche, M. Barkat, J.Colloid Interface Sci. 2006, 296, 434–441.
42. D.E. Bryant, D.I. Stewart, T.P. Kee, C.S. Barton, Environ. Sci. Technol. 2003, 37, 4011–4016
43. K.A. Venkatesan, V. Sukumaran, M.P. Antony, P.R.V. Rao, J. Radioanal. Nucl. Chem. 2004, 260, 443–450
44. S.B. Xie, C. Zhang, X.H. Zhou, J. Yang, X.J. Zhang, J.S. Wang, J. Environ. Radioactiv. 2009, 100, 162–166.
45. G. Tian, J.X. Geng, Y.D. Jin, C.L. Wang, S.Q. Li, Z. Chen, H. Wang, Y.S. Zhao, S.J. Li, J. Hazard. Mater. 2011, 190, 442–450.